ARTICLE

Electron Attachment Studies for $CHCl_3$ Using Ion Mobility Spectrometry

Hai-yan Han[a,b*], Hong-tao Feng[a], Hu Li[a], Hong-mei Wang[a], Hai-he Jiang[a], Yan-nan Chu[a]

a. Laboratory of Environmental Spectroscopy, Anhui Institute of Optics and Fine Mechanics, Chinese Academy of Sciences, Hefei 230031, China
b. College of Science, Hebei University of Engineering, Handan 060530, China

(Dated: Received on November 18, 2010; Accepted on January 12, 2011)

The dissociative electron attachment process for $CHCl_3$ at different electric field have been studied with nitrogen as drift and carrier gas using corona discharge ionization source ion mobility spectrometry (CD-IMS). The corresponding electron attachment rate constants varied from 1.26×10^{-8} cm^3/(molecules s) to 8.24×10^{-9} cm^3/(molecules s) as the electric field changed from 200 V/cm to 500 V/cm. At a fixed electric field in the drift region, the attachment rate constants are also detected at different sample concentration. The ion-molecule reaction rate constants for the further reaction between Cl^- and $CHCl_3$ are also detected, which indicates that the technique maybe becomes a new method to research the rate constants between ions and neural molecules. And the reaction rate constants between Cl^- and $CHCl_3$ are the first time detected using CD-IMS.

Key words: Ion mobility spectrometry, Dissociative electron attachment, Ion-molecule reaction rate constant, Chloroform

I. INTRODUCTION

The electron attachment rate constant to halocarbon molecules at low energy is an important parameter to investigate the kinetics for electronegative molecules in neural gas in many field including atmospheric chemistry in gaseous electronics and plasma process researches. The regular technique to measure electron attachment rate constants is negative mass spectrometry with different ionic methods such as electron swarm [1–3], threshold photoionization [4–6], electron cyclotron resonance [7, 8], the high-Rydberg atom beam [9, 10], crossed-beams [11], and flowing-afterglow Langmuir-prob [12, 13] techniques. All of these detect techniques are operated at vacuum system, which makes the technique become complex to manipulate and expensive to buy or set up.

In recent decades, ion mobility spectrometry (IMS) is used to invest the interactions between electrons and molecules at atmosphere. Ion mobility spectrometry was firstly introduced in the early 1970s. This technique has been developed as a trace analytical technique [14] based on the fact that ions have different drift velocities at ambient pressure as they move in a low electric field. The main advantages of IMS instruments are their high sensitivity, small size, and operation at atmospheric pressure, which makes that IMS have been widely applied in many fields, such as narcotics and explosives detection, environment pollution monitoring, disease diagnosis, structure analysis of clusters and biomolecules [15–19].

But the studies of the interactions between molecules and ions or electrons are not as rich as the sample detected using ion mobility spectrometry. After the IMS technique was invented, only several works introduced the electron attachment process for electronegative compounds by this technique. In 1973, Karasek *et al.* first investigated the interaction between electron and the electronegative molecules using negative ion mobility spectrometry [20]. Later Spangler *et al.* studied the electron capture rate constant for chlorobenzene using IMS technique in 1978 [21]. In 1998, the electron detachment of the molecules anion of azulene is studied by Sahlstrom *et al.* using IMS [22]. In 2004, Tabrizchi and coworkers investigated the electron attachment rate constants of three chloromethane compounds at different electric fields using CD-IMS [23]. In these studies, the electron attachment rate constant is obtained through the distribution of the sample ions in the drift region unlike the traditional electron swarm technique by which the data were obtained using the reduction of the electron current on the collector at the end of the drift tube.

In order to detect the detailed interaction process of the electronegative molecules with low energy electrons in IMS, we detected the electron attachment rate constants of $CHCl_3$ using the homemade corona discharge ion mobility spectrometry at different experimental conditions including the changing of the electric field in the drift region, the sample inlet position, the concentration of the sample. And the ion molecule reaction rate con-

*Author to whom correspondence should be addressed. E-mail: hanhy0226@163.com

stants between Cl^- and $CHCl_3$ are also detected using this technique.

II. EXPERIMENTS

The schematic diagram of the homemade corona discharge ion mobility spectrometer used in this work has been shown in Ref.[24]. The experimental apparatus mainly consists of the ionization source, reaction region, drift region, and detection system. In this experiment, the corona discharge ionization source has a point-to-plane geometry, and a typical discharge voltage on the corona needle is around 3 kV. The drift tube has a full length of 17 cm with internal diameter of 4 cm. The electrode rings of the drift tube are electronically insulated from each other by 1 mm thick Teflon spacer, and a high voltage is distributed through a series of resistors on these rings so that a uniform electric field along the axis of drift tube is formed. Another high voltage device is used to provide the electric field of both reaction and drift region. In order to detect the electron attachment rate constant at different electron energy, the electric field strength in the drift region is adjusted in the range of 200−500 V/cm. If a certain concentration of the high electronegativity sample molecules diffuses into the discharge region, the corona discharge maybe quenches. So there is a special electrode ring called curtain ring [23] after the discharge plate with a hole about 0.8 mm in the center of electrode ring. And the nitrogen gas entering the tube between the discharge plate and the curtain electrode ring is called curtain gas in order to provide the diffusion of the sample molecules into discharge region. The certain concentration of analyte is injected to the drift region by the drift gas from the end of drift tube. There is a shutter grid between the reaction region and the drift region, which consists of two series of parallel wires biased to a potential to create an orthogonal field relative to the drift field and can be switched periodically to inject the pulses of ions into the downstream drift tube. The ionic pulse width can vary from 100 μs to 200 μs. The ion current is collected by a faraday plate and an amplified signal is fed to the computer data processing system. The ion current versus the drift time is recorded as the ion mobility spectrum.

A syringe pump is used to make a certain concentration of the sample. The full mixture gas containing sample vapor gas and nitrogen is pulled into a glass micro-injector and injected into the drift gas by the syringe pump. The final concentration of the sample in the drift region can be calculated by the syringe pump speed, the initialization concentration and the flow rate of the drift gas. And the different sample concentration can be obtained by adjusting the pump speed and the flow rate of the drift gas. The drift and carrier gases used in these experiments are all high pure nitrogen gas (99.9995%), and the sample $CHCl_3$ is analytical reagent (99.97%).

III. RESULTS AND DISCUSSION

A. Theory

A swarm of electrons enter the drift tube and move to the collect plate under the influence of a uniform electric field in nitrogen gas. When the electronegative sample molecules are continuously introduced into the drift gas from the end of the drift tube, the neutral molecules M can capture electrons and the negative ions M^- are consequently generated in the drift region.

It is well known that the low energy electron attachment reaction to the halide organic compounds is a dissociative process, which dissociates to yield a negative halide Cl^- together with a neutral (usually a radical) fragment as reaction (1).

$$e + CHCl_3 \xrightarrow{k} CHCl_2 + Cl^- \tag{1}$$

The potential energy curves of the neutral $CHCl_3$ and the negative ion $CHCl_3{}^-$ and its dissociation into $CHCl_2$ and Cl^- versus the C−Cl separation have been given. The activation energy for electron direct attachment to a C−Cl bond in the stretching mode is estimated to be 0.07 eV [25].

The electron attachment rate of this reaction can be written as Eq.(2) according to the definition relation of the chemical reaction equation.

$$\frac{d[Cl^-]}{dt} = -\frac{d[e]}{dt} = k[RCl][e] \tag{2}$$

where [e] is the electron concentrations, [RCl] is the concentrations of neutral molecules $CHCl_3$, and $[Cl^-]$ is the concentration of Cl^-, respectively. The concentration of the Cl^- formed at each point in the drift region during the injection time of the electron swarm t_g [23] can be calculated by Eq.(3).

$$\left[Cl^-\right]_X = k\,[RCl]\,[e]_0\,t_g \exp\left[-\frac{k\,[RCl]\,v_d\,(t_d - t)}{w}\right] \tag{3}$$

where $[e]_0$ is the initial concentration of electrons, w is the electron velocity, v_d is the drift velocity of the ions, t_d is the drift time of the ion travel from the ion shutter grid to the collected plate, and t is the time of the ion spending from the point to the collected plate respectively. This equation shows the intensity of Cl^- ions generated in the drift region varying with the time when the $CHCl_3$ molecules are continuously introduced into the drift gas. This can form a tail signal before the corresponding ion peak. The logarithm of Eq.(3) is

$$\ln\left(\left[Cl^-\right]_X\right) = \ln\left(k\,[RCl]\,[e]_0\,t_g\right) - k\,[RCl]\,\frac{v_d t_d}{w} + k\,[RCl]\,\frac{v_d t}{w} \tag{4}$$

From Eq.(4), it can been seen that the logarithm of ion current intensity versus drift time for the tail before

DOI:10.1088/1674-0068/24/02/218-224

the corresponding ion peak is a straight line with a slope proportional to the rate constant, the first two terms are the intercept of the straight line and the last term is the slope of the line. If the ion velocity, the electron velocity and the sample concentration are known, the electron attachment rate constant can be easily obtained.

As the concentration of sample molecules is increased further, the chlorine ions can attach to the neutral sample molecules to become cluster ions as reaction (5),

$$Cl^- + RCl \xrightarrow{k_i} (RCl)\cdot Cl^- \tag{5}$$

As shown in Eq.(5), the number of cluster ions and their peak intensity in the mobility spectrum will be quantitatively proportional to the concentration of sample molecules. As the sample concentration is increased in the drift region, a second peak appears corresponding to RCl^- with a long drift time [26].

The reaction rate constant of reaction (5) can be written as:

$$\frac{d[(RCl)\cdot Cl^-]}{dt} = k_i[Cl^-][RCl] \tag{6}$$

The neutral sample molecules RCl are present in great abundance compared to product ions, thus, it is possible to assume that the sample concentration [RCl] is constant, so, just like Eq.(3), the concentration of $(RCl)\cdot Cl^-$ can be given by Eq.(7):

$$[(RCl)\cdot Cl^-]_X = k_i[RCl][Cl^-]_0 t_g \exp\left(\frac{-k_i[RCl]x}{V_{Cl^{-1}}}\right) \tag{7}$$

If the ions converting to $(RCl)\cdot Cl^-$ spend a fraction of time as being Cl^- and the other time as $(RCl)\cdot Cl^-$ ions in the drift region, the logarithm of the concentration of $(RCl)\cdot Cl^-$ can be obtained by Eq.(8) similar to Eq.(4):

$$\begin{aligned}\ln[(RCl)\cdot Cl^-]_t \;=\; & \ln\left(k_i[RCl][Cl^-]_0 t_g\right) - \\ & \frac{k_i[RCl]t_{Cl^-}t_{(RCl)\cdot Cl^-}}{t_{(RCl)\cdot Cl^-} - t_{Cl^-}} + \\ & \frac{k_i[RCl]t_{Cl^-}}{t_{(RCl)\cdot Cl^-} - t_{Cl^-}}t\end{aligned} \tag{8}$$

where t_g is the width of the Cl^- ions swarm passing through the drift region, t_{Cl^-} and $t_{(RCl)\cdot Cl^-}$ are the drift time of Cl^- and $(RCl)\cdot Cl^-$, respectively. If the Cl^- convert to $(RCl)\cdot Cl^-$ within the drift region, there is a tail between t_{Cl^-} and $t_{(RCl)\cdot Cl^-}$ in the mobility spectrum. From Eq.(8), it can be seen that the logarithm of the ion current intensity versus drift time for this tail is a straight line, and the slope of this line is the third item in Eq.(8) which is proportional to the rate constant k_i. Thus, utilizing slope value and the drift time for the Cl^- and $(RCl)\cdot Cl^-$, the rate constant can be easily obtained.

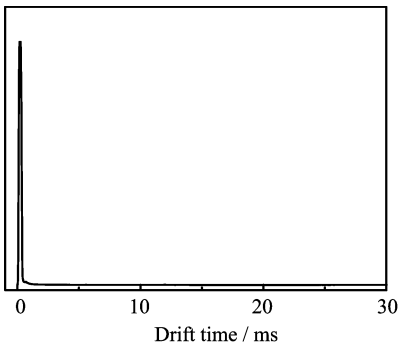

FIG. 1 The ion mobility spectrum of electron.

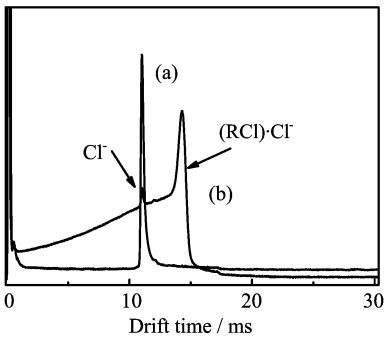

FIG. 2 The ion mobility spectrum of $CHCl_3$. (a) The sample was introduced into the ionization region and (b) the sample was introduced into the drift region.

B. Electron peak

In pure nitrogen, the electrons are effectively produced in the ion source and are extracted by the electric field and introduced into the reaction region. In the absence of sample molecules, the electrons pass through the reaction region practically without any chemical reactions and exhibit a distinct peak near zero drift time as illustrated in Fig.1.

C. Mobility spectra and rate constant

When the $CHCl_3$ molecules enter the reaction region before the ion shutter, the neutral molecules can capture the low-energy electrons to become Cl^- through reaction (1) and new ion peak appeared in the longer drift time domain in the mobility spectrum as illustrated in Fig.2(a), the background in this sepctrum is almost zero and no tail is found. The Cl^- is the dominant anion in this process as expected because the electron affinity of the Cl atom generally exceeds the C–Cl bond dissociation energy.

When a certain concentration of the sample is continuously carried into the drift region from the end of the drift tube by the drift gas, there is a tail at the arise edge of Cl^- peak in the mobility spectrum. This

DOI:10.1088/1674-0068/24/02/218-224

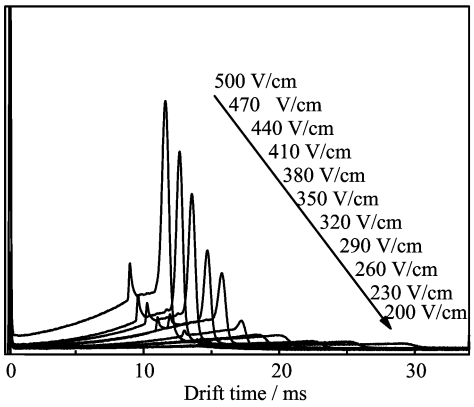

FIG. 3 The ion mobility spectrums $CHCl_3$ injected into the tube from the end of the drift region at various electric fields.

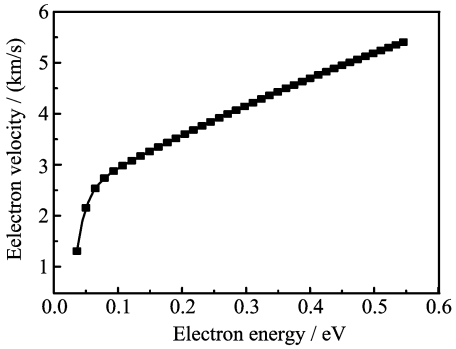

FIG. 4 The electron velocity curve varies with the electron energy.

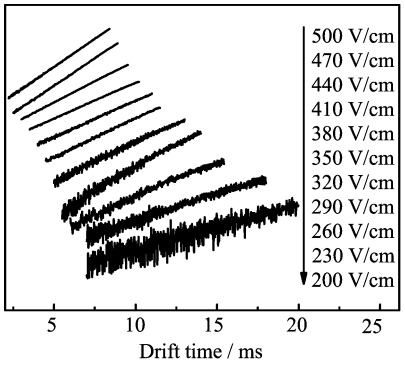

FIG. 5 Logarithm of the signal intensity for the negative ion tail before Cl^- when sample was injected into the tube from the end of the drift region at various electric fields of 200–500 V/cm.

tail corresponds to the Cl^- produced in the drift region as the molecules moving towards the shutter grid. The shape of this tail reflects the distribution of the Cl^- distribution in the drift region as presented in Fig.2(b). The peak at zero drift time corresponds to the electrons peak. The sample at the same concentration is detected at different drift electric fields from 200 V/cm to 500 V/cm, and the spectra are illustrated in Fig.3.

According to Eq.(4), the logarithm of the ion intensity of the tail plot varying with the drift time is expected to be a straight line, and the slope of this line equals to $k[\mathrm{RCl}]v_d/w$ on the basis of the last item. Using this relation of the slope and the rate constant, the electron attachment rate constant of $CHCl_3$ can be easily observed. In the item $k[\mathrm{RCl}]v_d/w$, the ion velocity w can be obtained through the ratio of the drift length and the drift time of the Cl^-, the electron velocity varying with the electron energy distribution can be obtained by the two exponential fitting line of the reference plots [27] illustrate in Fig.4. The electron energy at different electric field can be obtained through the electron energy distribution (E/N), which is determined by the electric field strength (E) divided by the number density (N) of the buffer gas. Using this method the electron attachment rate constants of $CHCl_3$ at different electric fields are obtained, the straight lines at different electric fields are illustrated in Fig.5. And the rate constant varying with the electron energy obtained in this work is given in Table I. The error of the data is within $\pm 0.05\times10^{-8}\mathrm{cm}^3/\mathrm{s}$, which is mainly caused by the concentration preparing process. From the data in Table I, it is can be seen that the electron attachment rate is a function of the electron energy, the rates exponential decay from 1.26×10^{-8} cm^3/s to 0.94×10^{-8} cm^3/s as the electron energy growing from 0.28 eV to 0.65 eV in the drift region. The rate constant values of $CHCl_3$ obtained in this work are compared with other reported data acquired by different methods in Refs.[23, 25], which are in good agreement with these data illustrated in Table I. There is a little difference between the two groups because of various experimental problems and the different methods applied.

And at a fixed drift field, the attachment rates of the sample with different concentration are also detected in this work. For example, the logarithm lines of the tails before Cl^- measured at 410 V/cm are illustrated in Fig.6. The slope of the line becomes larger as the sample concentration increasing, but the electron attachment rates are nearly a constant around 1.04×10^{-8} cm^3/s. This result proves that the electron attachment rate constant is not relative to the concentration of the sample but to the energy of the electrons in the drift region.

When the sample concentration is improved further, there are aggregation reactions or clustering reactions between Cl^- and neutral reagent chemical molecules happened in the drift region. In Fig.2 the second peak is corresponding to the cluster ions $(\mathrm{RCl})\cdot Cl^-$, the processing of this reaction has been described in reaction (5). The Gibbs energy of this reaction is about -36.366 kJ/mol small than other chloromethane (from -8.78 kJ/mol to -27.17 kJ/mol), which improves the opportunity of the clustering reaction [28]. The dissociation half-life of $(CHCl_3)\cdot Cl^-$ is 0.44 μs which is also larger than other chloromethanes with weaker associa-

DOI:10.1088/1674-0068/24/02/218-224

TABLE I Electron attachment constants k and ion molecular reaction constant k_i of $CHCl_3$ at deferent electron energy.

$(E/N)/(10^{-18}$ Vcm$^2)$	Electron energy/eV	$k/(10^{-8}$cm^3/s)			$k_i/(10^{-12}$cm^3/s)
		This work	Ref.[20]	Ref.[21]	
7.86	0.29	1.26	1.24	1.29	4.63
9.04	0.32	1.28	1.26		4.69
10.22	0.36	1.27	1.27	1.28	4.92
11.41	0.39	1.28	1.26		5.16
12.59	0.43	1.22	1.24	1.19	5.53
13.78	0.47	1.20	1.20		5.73
14.96	0.51	1.14	1.16		6.06
16.14	0.54	1.09	1.12	1.12	6.18
17.31	0.57	1.06	1.07		6.84
18.49	0.61	1.02	1.04	0.94	7.47
19.67	0.64	0.99	0.99		8.02

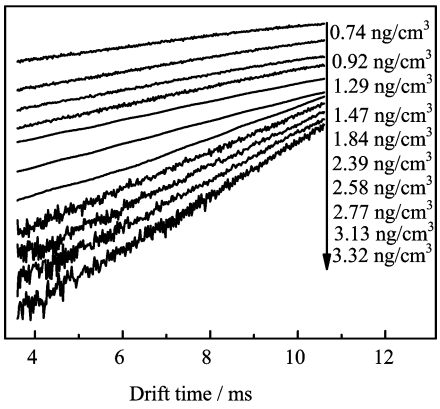

FIG. 6 The logarithm lines of the tails before Cl^- ions measured at different concentration with drift field at 410 V/cm.

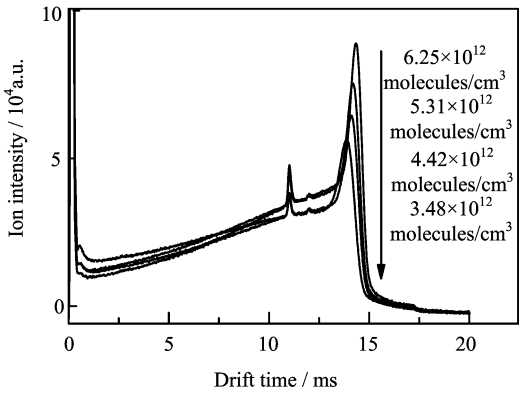

FIG. 7 The spectrums of four different concentration sample measured under the electric field at 410 V/cm.

tions with the Cl^- ion [29]. The tail between the Cl^- peak and the $(RCl)\cdot Cl^-$ peak in the spectrum is the mirror image of $(RCl)\cdot Cl^-$ ion distribution formed in the drift region through reaction (5). And the logarithm of the ion intensity during the tail plot versus the drift time is similar to Fig.5, which is expected to be a straight line according to Eq.(8), and the slope of this line is equal to $k_i[RCl]t_{Cl}/(t_{(RCl)\cdot Cl^-}-t_{Cl^-})$. Utilizing the slope value, the concentration of the neural sample molecules and the drift time for the Cl^- and $(RCl)\cdot Cl^-$, the clustering reaction rate constant k_i for reaction (5) can then be easily calculated. Using this method the reaction rate constant k_i at different electron field is obtained and illustrated in the last line of Table I. From the data, it is can be seen that the rate constant is a function of E/N, the rates exponential growth from 4.6×10^{-12} cm^3/s to 8.0×10^{-12} cm^3/s as the E/N growing from 7.85×10^{-18} Vcm^2 to 19.67×10^{-18} Vcm^2 in the drift region.

At a fixed drift field, the clustering reaction rates of $CHCl_3$ with Cl^- at different concentration are also detected. For example, the spectra of four different concentration sample measured under the electric field at 410 V/cm are shown in Fig.7. The peak at 11 ms has no changes in the drift time which corresponds to Cl^-. This phenomena is different from the result given by Tabrizchi *et al.* [23]. In that work, the drift time of Cl^- also shifts to the long time as the concentration increasing, maybe because of a small part of the neural sample molecular entering the reaction region. In our work, the drift time of Cl^- is a constant when the electric field is fixed whether the sample molecules enter the drift tube from the reaction region or from the drift region. But the peak around 14 ms corresponding to the cluster ions $(CHCl_3)\cdot Cl^-$ has a dramatic change in the drift time as the sample concentrations increasing. The magnitude of the shift of $(CHCl_3)\cdot Cl^-$ depends on the sample concentration in the drift region. The time of this peak shifts from 13.4 ms to 14.8 ms corresponding to the concentrations of $CHCl_3$ changing from 2.66×10^{11} molecule/cm^3 to 1.69×10^{12} molecule/cm^3. There are several reason causing the drift time shift to the longer time. The first reason is expected to the higher mass of the mixture drift gas instead of the pure nitrogen gas because of the

DOI:10.1088/1674-0068/24/02/218-224

magnitude $CHCl_3$ gas in the drift region, the mixture gas can improve the cross section of the $((CHCl_3)\cdot Cl^-$ with the neural drift gas. Eq.(9) is called mason-schamp equation [30], which describes the mobility of ions at a certain electric field in the neural drift gas.

$$K = \frac{3\sqrt{2\pi}}{16}\frac{q}{N}\sqrt{\frac{1}{\mu k_B T}}\frac{1+\alpha}{\Omega} \tag{9}$$

where q is the ionic charge, N is the number density of the neutral drift gas, k_B is the Boltzmann constant, T is the temperature, α is a small correction term with a magnitude of less than 0.02, when the ion mass is larger than the mass of the drift gas molecule, Ω is the average ion molecules collision cross section, and μ is reduced mass $mM/(m+M)$, m and M are the masses of the ion and the neutral molecule respectively. According to the mason-schamp equation, the mass of $(CHCl_3)\cdot Cl^-$ is lager than the mass of Cl^-, so the change for the collision cross section of $(CHCl_3)\cdot Cl^-$ and neural drift gas molecules is lager than that of Cl^- and neural drift gas. And Ω is changed as the concentration of sample increased in the drift tube, which makes the effect of changing of Ω for $(CHCl_3)\cdot Cl^-$ be also larger than that of Cl^-.

And another reason causing the drift time shift to the longer time is expected to the further clustering reactions for $(CHCl_3)\cdot Cl^-$ with other neural molecules in the drift region, *e.g.* H_2O and $CHCl_3$ molecules as the concentration improving as reaction (10) and reaction (11) [26].

$$(RCl)\cdot Cl^- + n(H_2O) \overset{k_c}{\longleftrightarrow} (RCl)\cdot Cl^-(H_2O)_n \tag{10}$$

$$(RCl)\cdot Cl^- + mRCl \overset{k_c}{\longleftrightarrow} (RCl)_{m+1}\cdot Cl^- \tag{11}$$

Both of the two reactions also have a high equilibrium constants at about 2.5×10^6 and 5.5×10^8 cm^3/s, respectively, which improves the opportunity of the clustering reactions [31, 32].

There is a small peak around 12 ms between the two peaks of $(CHCl_3)\cdot Cl^-$ and Cl^- as the spectrum in Fig.7, which corresponds to the ions of trace oxygen in the drift region [33]. The low-energy electrons can attach to oxygen molecules through three-body collisions to form $O_2{}^-$ the processing and the hydrates as shown in Eq.(12) to Eq.(14), where M can be N_2, O_2, and H_2O molecules. The relative degree of clustering depends on the temperature, water content, and reagent concentration of the system.

$$M + O_2 + e \rightarrow O_2{}^- + M \tag{12}$$

$$M + H_2O + O_2{}^- \rightarrow O_2{}^-H_2O + M \tag{13}$$

$$M + H_2O + O_2{}^-H_2O \rightarrow O_2{}^-(H_2O)_2 + M \tag{14}$$

In reasonably clean instrument gas, there are still traces of oxygen, water and other impurities present. The trance amount of O_2 and H_2O molecules exist in the drift region may be carried in by the impurity of the nitrogen gas and the sample preparing process. The peak shape in the spectrum is indicative of a rapidly achieved and dynamic equilibrium of mixture ions in which reversible reactions are fast relative to the time required for ion transit through the drift region. But this peak almost has no effect on the calculation process, because the intensity is much less than the intensity of $(CHCl_3)\cdot Cl^-$ ions which is just added on the intensity of the tail and can not affect the drift time of $(CHCl_3)\cdot Cl^-$ and the slope value of the straight.

IV. CONCLUSION

In this work the electron attachment rate constants for $CHCl_3$ are successfully obtained using negative corona discharge ion mobility spectrometry at the electric field varied from 200 V/cm to 500 V/cm. The ion-molecule reaction rates for Cl^- with $CHCl_3$ are also obtained from the tails between the Cl^- and $(CHCl_3)\cdot Cl^-$ in the spectrum. The electron attachment rate constants and ion-molecule reaction rates are also searched at different sample concentrations. The electron attachment rate constants data obtained in this work well agreed with the data reported in the different reference. And the ion-molecule reaction rate constants are first studied by negative corona discharge ion mobility spectrometry operating at ambient.

V. ACKNOWLEDGMENTS

The work was support by the National Natural Science Foundation of China (No.20707025 and No.20907054) and the Excellent Youth Foundation of Anhui Province Scientific Committee (No.06045098).

[1] A. A. Christodoulides and L. G. Christophorou, Chem. Phys. Lett. **61**, 553 (1979).
[2] S. R. Hunter, J. G. Carter, and L. G. Christophorou, J Chem. Phys. **90**, 4879 (1989).
[3] C. A. Mayhew, A. D. J. Ritchley, D. C. Howse, V. Mikhailov, and M. A. Parkes, Eur. Phys. J. D **35**, 307 (2005).
[4] A. Chutjian and S. H. Alajajian, Phys. Rev. A **31**, 2885 (1985).
[5] S. H. Lajajian and A. Chutjian, J. Phys. B **20**, 5567 (1987).
[6] S. H. Alajajian, K. F. Man, and A. Chutjian, J. Chem. Phys. **94**, 3629 (1991).
[7] S. F. Yoon, K. H. Tan, Rusli, and J. Ahn, J. Appl. Phys. **91**, 1634 (2002).
[8] O. Tuske, O. Delferriere, R. Gobin, F. Harrault, and T. Steiner, Rev. Sci. Instrum. **77**, 03A507 (2006).

DOI:10.1088/1674-0068/24/02/218-224

[9] C. B. Johnson, C. W. Walter, A. Kalamarides, K. A. Smith, and F. B. Dunning, J. Chem. Phys. **86**, 4945 (1987).
[10] T. Rauth, V. Grill, M. Foltin, P. Scheier, and T. D. Mark, J. Chem. Phys. **96**, 9241 (1992).
[11] S. Matejcik, G. Senn, P. Scheier, A. Kiendler, A. Stamatovic, and T. D. Mark, J. Chem. Phys. **107**, 8955 (1997).
[12] G. D. Sides, T. O. Tiernan, and R. J. Hanrahan, J. Chem. Phys. **65**, 1966(1976).
[13] T. M. Miller, J. R. Friedman, and A. A. Viggiano, Int. J. Mass. Spectrom. **267**, 190 (2007).
[14] R. H. Stlouis and H. H. Hill, Crit. Rev. Anal. Chem. **21**, 321 (1990).
[15] R. G. Ewing, D. A. Atkinson, G. A. Eiceman, and G. J. Ewing, Talanta **54**, 515 (2001).
[16] C. J. Koester and A. Moulik, Anal. Chem. **77**, 3737 (2005).
[17] Z. Karpas, B. Tilman, R. Gdalevsky, and A. Lorber, Anal. Chim. Acta **463**, 155 (2002).
[18] P. Weis, Int. J. Mass. Spectrom. **245**, 1 (2005).
[19] G. A. Eiceman, D. B. Shoff, C. S. Harden, A. P. Snyder, P. M. Martinez, M. E. Fleischer, and M. L. Watkins, Anal. Chem. **61**, 1093 (1989).
[20] F. W. Karasek, O. S. Tatone, and D. M. Kane, Anal. Chem. **45**, 1210 (1973).
[21] G. E. Spangler and P. A. Lawless, Anal. Chem. **50**, 290 (1978).
[22] K. E. Sahlstrom, W. B. Knighton, and E. P. Grimsrud, Int. J. Mass. Spectrom. **180**, 117 (1998).
[23] M. Tabrizchi and A. Abedi, J. Phys. Chem. A **108**, 6319 (2004).
[24] H. Y. Han, H. M. Wang, H. H. Jiang, M. Stano, M. Sabo, S. Matejcik, and Y. N. Chu, Chin. J. Chem. Phys. **22**, 605 (2009).
[25] T. Sunagawa and H. Shimamori, Int. J. Mass. Spectrom. **205**, 285 (2001).
[26] K. Giles and E. P. Grimsrud, J. Phys. Chem. **97**, 1318 (1993).
[27] G. K. Jarvis, R. A. Kennedy, and C. A. Mayhew, Int. J. Mass. Spectrom. **205**, 253 (2001).
[28] R. C. Doughert and J. D. Roberts, Org. Mass. Spectrom. **8**, 81 (1974).
[29] R. G. Ewing, G. A. Eiceman, and J. A. Stone, Int. J. Mass. Spectrom. **193**, 57 (1999).
[30] H. E. Revercomb and E. A. Mason, Anal. Chem. **47**, 970 (1975).
[31] K. Hiraoka, S. Mizuse, and S. Yamabe, J. Phys. Chem. **92**, 3943 (1988).
[32] K. Hiraoka, T. Mizuno, T. Iino, D. Eguchi, and S. Yamabe, J. Phys. Chem. A **105**, 4887 (2001).
[33] J. Stockdal, L. Christop, and G. S. Hurst, J. Chem. Phys. **47**, 3267 (1967).

DOI:10.1088/1674-0068/24/02/218-224